CHEM. RES. CHINESE UNIVERSITIES 2009, 25(6), 781—785

Preparation and Visible-light Photocatalytic Activity of Mesoporous $H_3PW_{12}O_{40}/TiO_2$ Composite

KANG Wan-li[1], LI Jin-huan[2], HUANG Jian-bin[1*], YU Xiao-dan[3] and GUO Yi-hang[3*]

1. State Key Laboratory for Structural Chemistry of Unstable and Stable Species, College of Chemistry and Molecular Engineering, Peking University, Beijing 100871, P. R. China;

2. Key Laboratory for Enhanced Oil Recovery, Ministry of Education, Daqing Petroleum Institute, Daqing 163318, P. R. China;

3. School of Chemistry, Northeast Normal University, Changchun 130024, P. R. China

Abstract Wormhole-like mesostructured $H_3PW_{12}O_{40}/TiO_2$ composite catalyst was prepared by the combination of sol-gel chemistry and solvothermal treatment technique in the presence of a triblock copolymer surfactant. Results of Raman spectra, XRD, BJH pore distribution and TEM image indicate that the composite possess a three-dimensionally interconnected pore mesostructure with a high porosity and large pore size. Keggin units were homogeneously dispersed throughout the composite. This composite can catalyze the photodegradation of crystal violet (CV) under visible-light. The photocatalytic activity is much higher than that of pure TiO_2 or $H_3PW_{12}O_{40}/TiO_2$ composite prepared in the absence of the surfactant.

Keywords Nanostructure; Mesoporous material; Photocatalysis

Article ID 1005-9040(2009)-05-781-05

1 Introduction

Design and preparation of visible-light-driven photocatalyst for the degradation of organic pollutants in waste water has attracted increasing attention. Anatase TiO_2 and polyoxometalates(POM) are two kinds of widely investigated photocatalytic materials. They have very similar photocatalytic processes owing to their similar electronic attributes[1—3]. The shortcoming of these two materials is that they have to be photoactivated by <380 nm light due to their high energy band gap, which makes use of solar light difficult since the solar light is mainly visible in a wavelength range of 400—800 nm. Recently, numerous efforts have been made in order to improve the photoefficiency of TiO_2 or POM on waste water under visible light[4]. It has been found that the fast photogenerated charge-pair(h^+-e^-) recombination on the surface of TiO_2 can be retarded by mixing a homogeneous POM(*e. g.*, $H_3PW_{12}O_{40}$, $H_4SiW_{12}O_{40}$ or $Na_4W_{10}O_{32}$) with a TiO_2 photocatalytic system. This results in the enhanced quantum efficiency of TiO_2 as a consequence of synergistic effect between TiO_2 and POMs[5]. Because POMs are strong electron acceptors, they are able to enhance the rate of conduction band electron transfer by accepting electrons from donors into its empty *d* orbits. Accordingly, the fast recombination rate of h^+-e^- pairs is retarded. In the $H_3PW_{12}O_{40}/TiO_2$ system, $H_3PW_{12}O_{40}$ can assist in the generation of the photogenerated oxidizing species because of its effective electron scavenging from the conduction band of TiO_2, consequently, it enhances the photocatalytic redox processes. As for the surfactant-templated mesoporous $H_3PW_{12}O_{40}/TiO_2$ composites, the pores are formed due to the structure directing function of the template, which creates the pores with 3D sponge-like mesostructrue and larger pore size. This pore morphology would minimize the diffusion of large dye molecules and increase pore accessibility. Our previous work has demonstrated porous TiO_2-based Keggin- and Dawson-type POM-containing composite catalysts have visible-light photocatalytic activity for the degradation of an organophosphorous pesticide[6]. These composite catalysts were prepared in the absence of the structure directing reagent. The pores in these materials are formed due to aggregation of the catalyst particles, which results in heterogenous pore sizes and low porosities. This less-controlled mesostructure results in less available active sites, which lowers the photocatalytic efficiency

---

*Corresponding author. E-mail: jbhuang@pku.edu.cn; guoyh@nenu.edu.cn

Received December 16, 2008; accepted January 30, 2009.

Supported by the National Natural Science Foundation of China(Nos.20633010 and 20873181), and the Program of New Century Excellent Talents in University, China(No.NCET-04-0311).

of these composites.

In this article, the authors report a new route, the combination of sol-gel chemistry and solvothermal treatment, to fabricate POM-TiO_2 composite catalysts with a high photocatalytic activity. Mesoporous $H_3PW_{12}O_{40}/TiO_2$ composite with unique surface physicochemical property was prepared in the presence of triblock copolymer surfactant pluronic P123 [$EO_{20}PO_{70}EO_{20}$, where EO=—CH_2CH_2O—, PO= —$CH_2CH(CH_3)O$—]. The photocatalytic activity of $H_3PW_{12}O_{40}/TiO_2$ composite on the degradation of crystal violet under visible-light was found as high as 90%.

2 Experimental

2.1 Materials

Titanium(IV) isopropoxide(TTIP, 98%) was purchased from J & K Chemical Inc., Beijing, China. 12-Tungstophosphoric acid(99.9%) and triblock copolymer surfactant(P123) were purchased from Aldrich Company, USA. Isopropyl alcohol(*i*-PrOH) and crystal violet(CV) were all A. R. grade agents and purchased from Beijing Chemical Company, China. All the reagents were used without further purification. Double distilled water was used throughout the experimental procedures.

2.2 Preparation of Catalyst Composite

Typically, 1.0 g of P123 was added into 20.0 mL of isopropenol(*i*-PrOH). The mixture was stirred for 1 h until the solid P123 was completely solublized, to which 4 mL of 98% titanium isopropoxide(TTIP) was then added. This mixture was homogenized and mixed with a $H_3PW_{12}O_{40}$ solution that was obtained by sonication of 0.12 g $H_3PW_{12}O_{40}$ in water(0.6 mL)/*i*-PrOH (2 mL) mixed solvent. This $H_3PW_{12}O_{40}$ solution was added dropwisely under vigorously stirring into the above P123/TTIP/*i*-PrOH system. Then the final mixture was adjusted to pH 2—3 by 12 mol/L HCl and stirred at room temperature till the formation of a clear hydrogel. The hydrogel was then put into an autoclave and heated to 100 °C at a heating rate of 2 °C/min. The temperature in the autoclave was kept for 48 h. After that, the gel was allowed to dehydrate slowly at 45 °C in vacuum for 24 h, 60 °C for 12 h, 80 and 100 °C for 2 h, and 120 °C for 0.5 h, respectively. Finally, the dry gel particulate was refluxed for 2 h in boiling absolute ethanol(30 mL×3) to ensure complete removal of the surfactant. The product was further calcinated at 400 °C for 1 h. The final product was denoted as $H_3PW_{12}O_{40}/TiO_2$. Pure TiO_2 and $H_3PW_{12}O_{40}/TiO_2$ composite in the absence of P123 (denoted as $H_3PW_{12}O_{40}/TiO_2$-D) were also prepared similarly.

2.3 Characterization Methods

Loading percentage of $H_3PW_{12}O_{40}$ for $H_3PW_{12}O_{40}/TiO_2$ and $H_3PW_{12}O_{40}/TiO_2$-D were *ca*. 8.6%(mass fraction), which were determined by a Leeman Prodigy ICP-AES. Raman spectra were recorded on a Jobin-Yvon HR 800 instrument with an Ar^+ laser source of 488 nm wavelength in a macroscopic configuration. UV-Vis/DRS spectra were recorded on a Cary 500 UV-Vis-NIR spectrophotometer. Low and wide-angle XRD patterns were recorded on a Rigaku D/Max-3C X-ray diffractometer. TEM image was obtained on a JEOL JEM-2010 transmission electron microscope at an accelerating voltage of 200 kV. BET specific surface areas and BJH pore sizes were calculated from N_2 adsorption/desorption isotherms determined at −196 °C on an ASAP 2010M porosimeter. X-ray photoelectron spectroscopy(XPS) was performed on a VG-ADES 400 instrument with Mg *Kα* ADES source at a residual gas pressure of below 10^{-8} Pa.

2.4 Photocatalytic Test

The suspension including CV and $H_3PW_{12}O_{40}/TiO_2$ was ultrasonicated for 10 min and stirred in the dark for 30 min before visible-light irradiation. Afterwards, a Xe lamp(400 W, λ >420 nm) was inserted into the suspension to initiate the photocatalytic reaction. The temperature of the suspension was kept at (30±2) °C by circulation water through an external cooling coil and the system was open to air. During the process of the photocatalytic test, the concentration of CV was monitored by a Cary 500 UV-Vis-NIR spectrophotometer at λ=583 nm after centrifugation and filtration of the suspension. Changes of total organic carbon(TOC) in the reaction system were monitored *via* a Shimadzu TOC-500 Total Organic Carbon analysis system.

3 Results and Discussion

3.1 Structure of Photocatalyst

The structure of the synthesized photocatalyst was first investigated by Raman spectra since the

Keggin units are extremely sensitive to Raman scattering in the composite. Fig.1 shows the Raman spectra of the $H_3PW_{12}O_{40}/TiO_2$ composite, starting TiO_2 and $H_3PW_{12}O_{40}$ material. The starting Keggin units show four Raman scattering peaks in the range of 1100—900 cm^{-1}, which are attributed to the stretching vibrations of the P—O bonds of PO_4 sites(1007.0 cm^{-1}), W═O bonds(988.6 cm^{-1}) and W—O—W bonds(920.6 and 887.3 cm^{-1}) of the Keggin units, respectively. After the formation of the $H_3PW_{12}O_{40}/TiO_2$ composite, the scattering peak intensities decreased significantly, at the same time, the corresponding peaks shift to 994.6, 984.8, and 887.4 cm^{-1}, respectively. The result indicates that the primary Keggin structure remains intact, and there exists a strong interaction between the Keggin unit and titania support[7]. This is attributed to the well-matched electronegativity and ionic radius of Ti^{4+}(1.54, 0.0605 nm) and W^{6+}(1.70, 0.060 nm). After incorporation of $H_3PW_{12}O_{40}$ into anatase TiO_2 crystal lattice, scattering peaks corresponding to W—O—W, W═O, and P—O bond vibrations are broadened, these changes are due to the strong interaction between the Keggin unit and anatase TiO_2 framework.

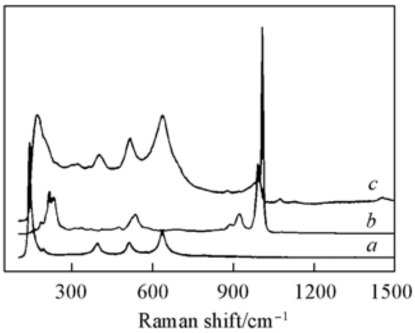

Fig.1 Raman spectra of starting TiO_2(*a*), $H_3PW_{12}O_{40}$(*b*) and as-prepared $H_3PW_{12}O_{40}/TiO_2$(*c*) composite

Wide-angle XRD analysis was employed to study the phase type of the $H_3PW_{12}O_{40}/TiO_2$ composite. As shown in Fig.2, the composite has a similar XRD pattern as that of directly prepared $H_3PW_{12}O_{40}/TiO_2$-D, which indicates the as-prepared $H_3PW_{12}O_{40}/TiO_2$ composite is mainly anatase phase. The small peak situated at 30.8° is assigned to brookite TiO_2 phase(JCPDS No. 29-1360). In addition, no features of $H_3PW_{12}O_{40}$ crystalline phase were found in both the composites, indicating homogeneously dispersed Keggin units throughout the composite. In the low-angle region, one broader reflection peak of (100) at 0.83°(inset of Fig.2) appears, which is in good agreement with the material prepared by a neutral template[8], thus indicates that the $H_3PW_{12}O_{40}/TiO_2$ composite owns a wormhole-like unordered mesoporous structure[8].

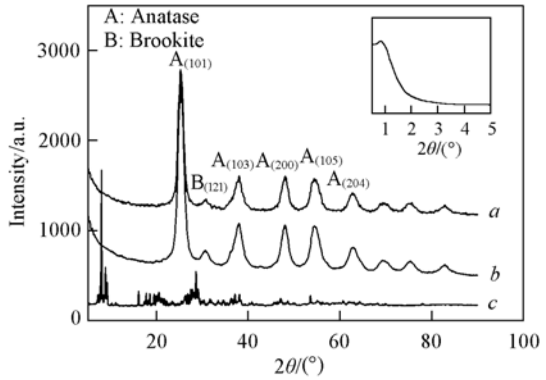

Fig.2 Wide- and low-angle(insert) XRD patterns of $H_3PW_{12}O_{40}/TiO_2$ composite

2θ values for the two composites are 25.3°(101), 37.9°(103), 48.0°(200), 54.6°(105), and 62.8°(204), respectively.

a. $H_3PW_{12}O_{40}/TiO_2$-D; *b*. $H_3PW_{12}O_{40}/TiO_2$; *c*. $H_3PW_{12}O_{40}$.

Although the crystal phase types are almost the same for composites prepared with and without P123 surfactant, the UV-Vis/DRS results(Fig.3) show that a small red shift occurs for the absorption of the $H_3PW_{12}O_{40}/TiO_2$ composite compared with the absorption from $H_3PW_{12}O_{40}/TiO_2$-D composite. This result indicates that the local Keggin units in the former are different from those in the latter. In addition, no solitary absorption peak related to the Keggin units is found in both the composites, which confirms the presence of homogeneously dispersed Keggin units throughout the composites.

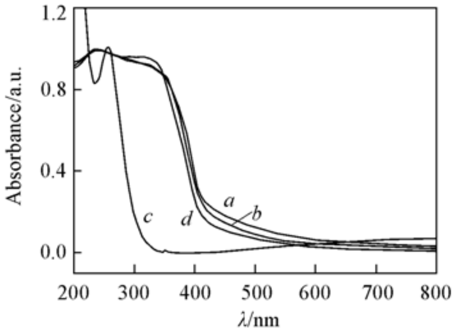

Fig.3 UV-Vis/DRS spectra of TiO_2, starting $H_3PW_{12}O_{40}$ and $H_3PW_{12}O_{40}/TiO_2$ composite

a. TiO_2; *b*. $H_3PW_{12}O_{40}/TiO_2$; *c*. $H_3PW_{12}O_{40}$; *d*. $H_3PW_{12}O_{40}/TiO_2$-D.

The indication of the change of the local environment for the Keggin units in the composite prepared in the presence of P123 surfactant drove us to analyze the surface tungstate environment as a function of $H_3PW_{12}O_{40}$ loading *via* XPS. The W_{4f} XPS results of $H_3PW_{12}O_{40}/TiO_2$ and the pure parent $H_3PW_{12}O_{40}$(calcined 100 °C) are shown in Fig.4. The spectra reveal a broad, poorly resolved doublet centre around 35.3 eV($4f_{7/2}$ component) in the XPS of W_{4f} region in $H_3PW_{12}O_{40}/TiO_2$. The bands are shifted markedly to a lower binding energy at 35.8 eV for $W_{4f_{7/2}}$ in the pure parent $H_3PW_{12}O_{40}$ heteropoly acid. The lower binding energy tungstate in the $H_3PW_{12}O_{40}/TiO_2$ suggests that this species is associated with the titania interface. Newman *et al.*[9] investigated the surface environment and structural evolution of silica supported phosphotungstic acid ($H_3PW_{12}O_{40}$) catalysts. They proposed that the intimate contact of $H_3PW_{12}O_{40}$ with the silica matrix perturbed the local chemical environments of the three tungstate centres in the Keggin unit; then the environments of these tungstate centers become different from those of the tungstate centers in the remaining cluster, as is indicated by the variation of the adsorption mode of the three terminal W═O groups. Analogously, the negative shifts in binding energies of the W_{4f} states in our composite are ascribed to the reduction of tungsten ions[9].

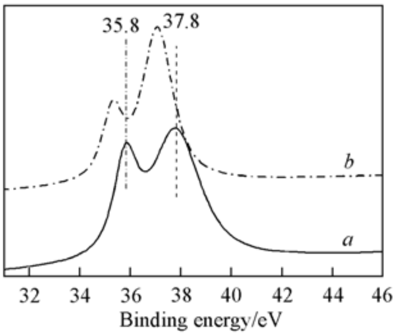

Fig.4 High-resolution XPS of W_{4f} region in HPW preheated(100 °C) and $H_3PW_{12}O_{40}/TiO_2$ composites

a. $H_3PW_{12}O_{40}$; *b*. $H_3PW_{12}O_{40}/TiO_2$.

The overall mesoporosity of $H_3PW_{12}O_{40}/TiO_2$ was examined by N_2 porosimetry(Fig.5). It is Type IV with H2-type hysteresis loop, and the adsorbed N_2 amount increases rapidly at p/p_0 from 0.4 to 0.7. This is an indication of three-dimensionally interconnected porous structure of the composite. The narrow pore-size distribution(inset of Fig.5) implies that the pores of the composites are formed within TiO_2 framework rather than voids among the particles. The calculated BET surface areas for $H_3PW_{12}O_{40}/TiO_2$ and $H_3PW_{12}O_{40}/TiO_2$-D are 158.9 and 151.5 m^2/g, respectively, much larger than that of pure $H_3PW_{12}O_{40}$. Moreover, both the pore volume(0.20 cm^3/g) and average pore diameter(5.0 nm) of the $H_3PW_{12}O_{40}/TiO_2$ are larger than the corresponding ones of the $H_3PW_{12}O_{40}/TiO_2$-D(0.15 cm^3/g and 2.9 nm, respectively).

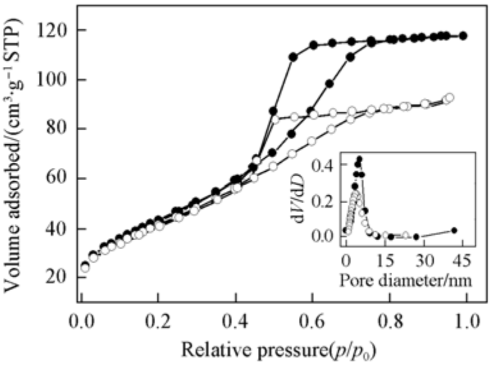

Fig.5 N_2 adsorption/desorption isotherms and pore size distribution curves(inset) of mesoporous $H_3PW_{12}O_{40}/TiO_2$ composites

● $H_3PW_{12}O_{40}/TiO_2$; ○ $H_3PW_{12}O_{40}/TiO_2$-D.

The three-dimensionally interconnected porous structure of $H_3PW_{12}O_{40}/TiO_2$ composite was also revealed by TEM observation(Fig.6). The pores connect randomly and are lack of discernible long-range order. This result is in good agreement with that of low-angle XRD or N_2 porosimetry. Formation of this highly porous structure with controllable pore size is associated with the roles of the surfactant and $H_3PW_{12}O_{40}$[10]. $H_3PW_{12}O_{40}$ is favorable for forming a stable sol-gel network with an ordered array of Ti and O without leading to the shrinkage and collapse of the network[11]. The surfactant P123 can disperse the product particles homogeneously, thereby reduce aggregation among particles.

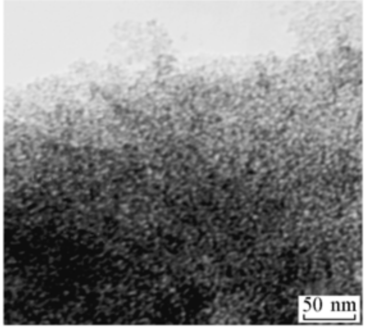

Fig.6 TEM image of mesoporous $H_3PW_{12}O_{40}/TiO_2$ composites

3.2 Photocatalytic Test

The photocatalytic activity of $H_3PW_{12}O_{40}/TiO_2$ was evaluated with CV dye degradation test under visible-light irradiation(Fig.7). Degradation of CV was hardly detected after 6 h irradiation of a CV solution under visible-light. In the presence of pure TiO_2, a very slow degradation of CV was observed. However, significant degradation of CV occured in the presence of $H_3PW_{12}O_{40}/TiO_2$ or $H_3PW_{12}O_{40}/TiO_2$-D composite. Catalyzed by the $H_3PW_{12}O_{40}/TiO_2$ photocatalyzed system, the conversion rate of CV after 3 h visible light irradiation is as high as 90.0%, whereas under the identical conditions, the conversion rate of CV catalyzed by the $H_3PW_{12}O_{40}/TiO_2$-D catalyzed system is 71.0%. Obviously, $H_3PW_{12}O_{40}/TiO_2$ composite is much more effective than $H_3PW_{12}O_{40}/TiO_2$-D for the photocatalysis degradation of CV.

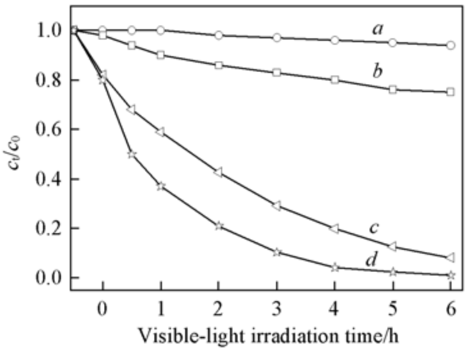

Fig.7 Visible-light photodegradation of dye CV(25 mg/L, 100 mL) over different catalysts(250 mg)

a. Direct photolysis; *b*. pure TiO_2; *c*. $H_3PW_{12}O_{40}/TiO_2$-D; *d*. $H_3PW_{12}O_{40}/TiO_2$.

The high photocatalytic activity of $H_3PW_{12}O_{40}/TiO_2$ compared with TiO_2 is due to the synergistic effect between $H_3PW_{12}O_{40}$ and anatase TiO_2, which results in the enhancement of composition quantum efficiency[6]. Recently, polyoxometalates(POMs) have been applied to TiO_2 photocatalytic systems as electron scavengers to retard the fast charge-recombination with h^+ in TiO_2 and, consequently, it enhances the photocatalytic redox processes[12—17]. The much higher photocatalytic activity of $H_3PW_{12}O_{40}/TiO_2$ with respect to $H_3PW_{12}O_{40}/TiO_2$-D is related to the surfactant templating effect, which ensures the larger surface area, pore volume and size. Upon comparison of the pore parameters in the two composites' systems, one may find that the catalysis activity increases approximately proportionally to the pore volume(91% over 71% for the activity, and 0.20 cm^3/g over 0.15 cm^3/g). It is probably that, the larger interconnected pore volume and the uniform pore size distribution in the $H_3PW_{12}O_{40}/TiO_2$ composite are of advantage for CV molecules diffusion. In addition, the high porosity of the composite also gives rise to a higher population of available active sites. Both favor a higher photocatalytic efficiency.

4 Conclusions

Mesoporous $H_3PW_{12}O_{40}/TiO_2$ composite was prepared by combination of sol-gel and solvothermal treatment technique in the presence of P123 surfactant template. Kiggen units of $H_3PW_{12}O_{40}$ were homogenously dispersed in the TiO_2 matrix. The $H_3PW_{12}O_{40}/TiO_2$ composite shows analogous anatase phase structure to that of composite prepared in the absence of P123, but the local environment of the tungstate is modified by the present P123 surfactant. The composite has an exhibited high visible-light photocatalytic activity to dye CV degradation. This enhanced photocatalytic activity is attributed to the narrow pore size distribution, larger pore volume and area, and higher porocity brought about the present P123 surfactant.

References

[1] Kormali P., Troupis A., Triantis T., *et al.*, *Catal. Today*, **2007**, *124*, 149

[2] Liu H., Yuan J., Shangguan W. F., *Chem. J. Chinese Universities*, **2008**, *29*(8), 1603

[3] Wei Z. G., Zhang H. X., Li Q. S., *et al.*, *Chem. J. Chinese Universities*, **2008**, *29*(4), 824

[4] Guo Y., Hu C., Wang X., *et al.*, *Chem. Mater.*, **2001**, *13*, 4058

[5] Ozer R. R., Ferry J. L., *J. Phys. Chem. B*, **2002**, *106*, 4336

[6] Li L., Wu Q., Guo Y., *et al.*, *Micropor. Mesopor. Mater.*, **2005**, *87*, 1

[7] Guo Y., Li K., Yu X., *et al.*, *Appl. Catal. B*: *Environ.*, **2008**, *81*, 182

[8] Lee B., Yamashita T., Lu D., *et al.*, *Chem. Mater.*, **2002**, *14*, 867

[9] Yu J., Su Y., Cheng B., *et al.*, *J. Mol. Catal. A*, **2006**, *258*, 104

[10] Choi H., Sofranko A. C., Dionysiou D. D., *Adv. Funct. Mater.*, **2006**, *16*, 1067

[11] Huang D., Wang Y. J., Yang L. M., *et al.*, *Micropor. Mesopor. Mater.*, **2006**, *96*, 301

[12] Yoon M., Chang J. A., Kim Y., *et al.*, *J. Phys. Chem. B*, **2001**, *105*, 2535

[13] Kim S., Park H., Choi W., *J. Phys. Chem. B*, **2004**, *108*, 6402

[14] Chen C., Lei P., Ji H., *et al.*, *Environ. Sci. Technol.*, **2004**, *38*, 329

[15] Ozer R., Ferry J., *Environ. Sci. Technol.*, **2001**, *35*, 3242

[16] Yang Y., Guo Y., Hu C., *et al.*, *Appl. Catal. A*, **2003**, *252*, 305

[17] Kiwi J., Grätzel M., *J. Phys. Chem.*, **1987**, *91*, 6673